FEBS Letters 588 (2014) 1016–1023

journal homepage: www.FEBSLetters.org

Characterization of bacterial NMN deamidase as a Ser/Lys hydrolase expands diversity of serine amidohydrolases

Leonardo Sorci [a], Lucia Brunetti [b], Lucia Cialabrini [b], Francesca Mazzola [a], Marat D. Kazanov [c], Sabato D'Auria [d], Silverio Ruggieri [b], Nadia Raffaelli [b,*]

[a] Department of Clinical Sciences, Polytechnic University of Marche, Ancona, Italy
[b] Department of Agricultural, Food and Environmental Sciences, Polytechnic University of Marche, Ancona, Italy
[c] A.A. Kharkevich Institute for Information Transmission Problems, Russian Academy of Sciences, Moscow, Russia
[d] Laboratory for Molecular Sensing, IBP-CNR, Napoli, Italy

ARTICLE INFO

Article history:
Received 6 December 2013
Revised 23 January 2014
Accepted 26 January 2014
Available online 11 February 2014

Edited by Miguel De la Rosa

Keywords:
NMN deamidase
Pyridine nucleotide
Catalytic dyad
Amidohydrolase
Site-directed mutagenesis

ABSTRACT

NMN deamidase (PncC) is a bacterial enzyme involved in NAD biosynthesis. We have previously demonstrated that PncC is structurally distinct from other known amidohydrolases. Here, we extended PncC characterization by mutating all potential catalytic residues and assessing their individual roles in catalysis through kinetic analyses. Inspection of these residues' spatial arrangement in the active site, allowed us to conclude that PncC is a serine-amidohydrolase, employing a Ser/Lys dyad for catalysis. Analysis of the PncC structure in complex with a modeled NMN substrate supported our conclusion, and enabled us to propose the catalytic mechanism.

1. Introduction

Amidohydrolases represent a numerous group of hydrolases acting on amide carbon–nitrogen bonds. They are categorized under EC numbers 3.4 and 3.5, according to whether they act on peptide bonds (peptidases and proteases) or other carbon–nitrogen bonds. Amidohydrolases comprise thousands of members with diverse chemistry and functional roles. The salient mechanistic hallmark of these enzymes is the structure-aided activation of a nucleophile, either a water molecule or aminoacid side chain, that can attack the amide group for cleavage. The water molecule activation can be achieved through complexation with a mononuclear or binuclear metal center as in metalloproteases [1], or by interaction with an acid residue in conjugate base form as in aspartate/glutamate proteases [2]. In other cases, a serine, threonine, or cysteine residue acts as the major nucleophile after its activation triggered by one or more conserved residues in the active site. In this latter group, a covalent acyl-enzyme intermediate is generated. The first identified and most studied active site architecture is the "classic" Ser/His/Asp catalytic triad of serine proteases [3]. Subsequently, variations of this characteristic triad have been reported, either in the residues' identity, like the Ser/Ser/Lys triad characterizing the "amidase signature superfamily" [4,5], or in the number of participating residues, as seen in the dyads or in the Ser-only configurations [6].

Recently, we have identified and functionally characterized a novel member of the amidohydrolase group, the enzyme nicotinamide mononucleotide (NMN) deamidase (PncC, EC 3.5.1.42), formerly known as Competence/damage-inducible protein CinA [7]. PncC catalyzes the hydrolysis of the carbamide bond in the nicotinamide moiety of NMN yielding nicotinic acid mononucleotide (NaMN), a key intermediate in NAD biosynthetic pathway. Our previous study showed that PncC is both phylogenetically and structurally separate from other known amidohydrolases [7]. Indeed,

Abbreviations: NMN, nicotinamide mononucleotide; NaMN, nicotinic acid mononucleotide; NaAD, nicotinic acid adenine dinucleotide; HPLC, high pressure liquid chromatography; PMSF, phenylmethylsulfonylfluoride; CD, circular dichroism

* Corresponding author. Address: Via Brecce Bianche, 60131 Ancona, Italy. Fax: +39 0712204677.
E-mail address: n.raffaelli@univpm.it (N. Raffaelli).

http://dx.doi.org/10.1016/j.febslet.2014.01.063

PncC does not align with any characterized amidase sequence, nor contains a signature typical of known amidohydrolase families. Its three-dimensional structure, which is available for the apo-protein from *Agrobacterium tumefaciens*, as determined by the Midwest Center for Structural Genomics, represents a unique and distinctive fold. In the SCOP database it is classified as the only member of the CinA-like superfamily of amidohydrolases, here renamed as PncC superfamily.

In the present study, we combined mutational and structural analysis to gain insight into the PncC active site architecture. Our results point to a Ser/Lys dyad as a catalytic center for the PncC superfamily, as seen in several proteases [8,9] and some amidases [10,11]. Overall, these features characterize PncC as a novel example of convergent evolution.

2. Materials and methods

2.1. In silico analysis

PncC protein sequences (see Supplementary information) were retrieved from The SEED comparative genomics database (http://pubseed.theseed.org) [12]. Due the large number of sequences (760 at the time of the analysis), a final set of 447 sequences was obtained after removing fragments and redundancy among strains coming from the same species. Prior to the alignment using Muscle [13], the COG1058 domain of the bifunctional COG1058/PncC proteins [14] was manually removed. The most divergent sequences (30) were obtained by decreasing redundancy (85% max similarity threshold). Multiple sequence alignment and secondary structure elements were displayed using ESPript/ENDscript [15].

2.2. Site-directed mutagenesis and mutants' expression and purification

Site-directed mutagenesis of *Escherichia coli* PncC was carried out using the QuikChange XL Site-Directed Mutagenesis Kit (Agilent Technologies), according to the manufacturer's instructions. Sequences of mutagenic primers are listed in Table S1. The plasmid pCA24N-pncC, used as the PCR template, was purified from the *E. coli* ASKA clone [16]. The mutagenized plasmids were sequenced to verify incorporation of the desired modification and to ensure the absence of random mutations. For mutants and wild-type protein expression, the plasmids were transformed into electrocompetent *E. coli* BL21(DE3) cells. Cells were grown at 37 °C in Luria Bertani medium supplemented with 0.030 mg/ml chloramphenicol. After reaching an OD_{600} of 0.3, cultures were shifted at 25 °C and expression was induced with 1 mM isopropyl β-D-thiogalactopyranoside (IPTG), at an OD_{600} of 0.6. After 3 h induction, cells from 20-ml cultures were harvested by centrifugation at 5000×*g* for 10 min, resuspended in 1 ml buffer A (50 mM TRIS/HCl buffer, pH 7.5, 0.15 M NaCl, 1 mM DTT) containing 1 mM phenylmethylsulfonylfluoride (PMSF) and 0.002 mg/ml leupeptin, antipain and chymostatin. The suspensions were sonicated for 3 min at 50 watt, with 30 s intervals, and centrifuged at 15000×*g* for 30 min. The supernatants representing the soluble fractions and the corresponding pellets were analyzed by SDS–PAGE [17]. The soluble fractions containing the recombinant proteins were assayed for the enzymatic activity and applied to a 5-ml HisTrap HP column (GE Healthcare), equilibrated with buffer A, containing 10 mM imidazole. The column was washed with the equilibration buffer, and elution was performed with an imidazole gradient from 10 mM to 350 mM in buffer A. Fractions containing the recombinant proteins (eluted at about 100 mM imidazole) were pooled and purity of the preparations was assessed by SDS–PAGE. Pools were dialyzed against 50 mM TRIS/HCl buffer, pH 7.4, 0.15 mM NaCl, and used for the kinetic characterization.

2.3. PncC activity determination and kinetic experiments

NMN deamidase activity was measured with a continuous spectrophotometric assay, as described in [7]. Briefly, NaMN formation by the enzyme is coupled to the conversion of NaMN to NADH, in the presence of recombinant *E. coli* NadD (converting NaMN to NaAD), NadE (amidating NaAD to NAD) and yeast alcohol dehydrogenase. For kinetic analyses, the HPLC-based assay relying on direct quantitation of NaMN was used, as described [7]. Briefly, reaction mixtures contained 50 mM HEPES buffer, pH 7.5, NMN concentrations ranging from 1 μM to 3 mM, and appropriate amounts of purified proteins. After incubation at 37 °C, reactions were stopped with 0.6 M $HClO_4$, and after 10 min on ice, the samples were centrifuged for 1 min at 12000×*g*. The supernatants were neutralized with 0.8 M K_2CO_3, kept on ice for 10 min, and centrifuged as described above, before injection into an ion-paired analytical Supelcosil LC18-S column (5 μM, 4.6 × 250 mm). Elution conditions were 4 min at 100% buffer A (100 mM potassium phosphate, pH 6.0, 8 mM tetrabutylammonium hydrogen sulfate), 6 min up to 7% buffer B (buffer A containing 30% methanol), returning to 100% buffer A in 1 min, and holding at 100% buffer A for 5 min. The amount of enzyme in the reaction mixture was maintained at a level between 0.1 and 500 μg/ml, leading to 1–10% substrate consumption within the incubation time. The linearity of response was assessed by the analysis of aliquots taken at 2 time points (10 and 20 min) over the course of reaction. Apparent values of K_m and k_{cat} were calculated by fitting initial rates to a standard Michaelis–Menten model using the software Prism 4 (GraphPad).

2.4. PMSF and fluorophosphonate inhibition studies

The influence of PMSF and a biotynilated fluorophosphonate (Desthiobiotin-FP, Thermo Scientific, Rockford, IL USA) on PncC activity was tested by incubating the pure enzyme (final concentration 0.1 μg/ml) in the presence of 1.0 mM PMSF or 0.1 mM desthiobiotin-FP, and 1 mM NMN. At different incubation times at 37 °C, NaMN product was quantified using the HPLC assay described above.

2.5. Thermal stability assay

Purified T31A, E28A, and wild type PncC (final concentration 0.5 mg/ml) were incubated at 70 °C in 50 mM TRIS/HCl buffer, pH 7.4, 0.15 mM NaCl. Aliquots were taken at different times, and enzymatic activity was assayed as described above.

2.6. Circular dichroism analysis

CD measurements were performed on purified R142A, Y56A, and wild type PncC at protein concentration of 0.1 mg/ml for far-UV measurements and 0.3 mg/ml for near-UV measurements, in 2.0 mM Tris–HCl buffer, pH 7.4, at 25 °C. A spectropolarimeter model J-810 (Jasco, Tokyo, Japan) equipped with the temperature-controlled liquid systems Neslab RTE-110 (Neslab Instruments, Portsmouth, NH) calibrated with a standard solution of 10-camphor sulfonic acid was used. Circular quartz cuvettes (Helma, Jamaica, NY) with 0.1 cm and 0.5 cm path length were used for the measurements in the far-UV (200–250 nm) and near-UV

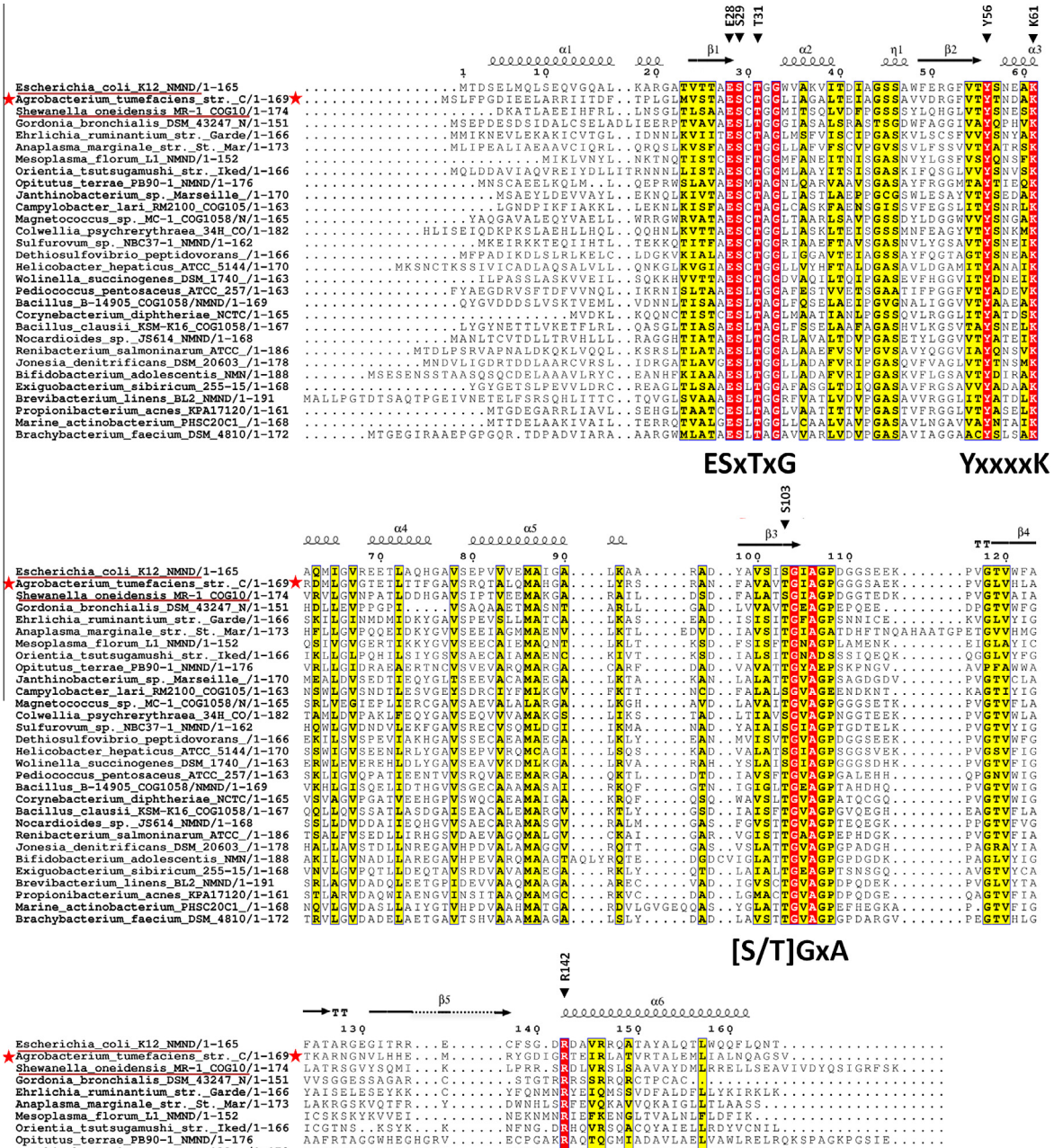

Fig. 1. Multiple sequence alignment for most divergent PncC proteins, including the experimentally characterized PncCs from *E. coli* strain K12 and *Shewanella oneidensis* MR-1 (underlined), and PncC from *Agrobacterium tumefaciens* strain C58, whose 3D structure is available (marked within stars). Mutated residues are indicated by arrows (*E. coli* sequence numbering). Conserved residues are marked with a red background. Less conserved residues are indicated with yellow background. Secondary structure elements of *at*PncC (PDB 2A9S) are also displayed: springs represent α-helices and arrows represent β-strands. The signature sequences are also shown.

(250–320 nm), respectively. A spectral acquisition spacing of 0.2 nm (1.0 nm bandwidth) was used in the far-UV region, and 0.1 nm spacing (1.0 nm bandwidth) in the near-UV region. Photomultiplier absorbance did not exceed 500 V in the spectral regions measured. Each spectrum was averaged ten times and smoothed with Spectropolarimeter System Software Ver. 1.00 (Jasco). All measurements were performed under nitrogen flow. The results are expressed in terms of ellipticity (millidegree).

Table 1
Kinetic analyses of wild-type and *ec*PncC mutants.

Mutated residue in *ec*PncC[a]	*at*PncC numbering	k_{cat} (s^{-1})	K_m (μM)	k_{cat}/K_m (s^{-1} mM^{-1})
None		4.1 ± 0.2	7 ± 2	$5.9 \cdot 10^2$
E28	E30	3.9 ± 0.2	272 ± 38	$0.1 \cdot 10^2$
S29	S31	ND[b]	–	–
T31	T33	3.2 ± 0.2	27 ± 2	$1.2 \cdot 10^2$
Y56	Y58	ND[b]	–	–
K61	K63	ND[b]	–	–
S103	T105	1.1 ± 0.2	12 ± 3	$0.9 \cdot 10^2$
R142	R145	ND[b]	–	–

[a] All residues have been mutated to alanine, with the exception of K61 that was engineered to glutamine. Kinetic parameters were determined as described in Section 2.
[b] ND, not detectable.

3. Results and discussion

3.1. Identification of PncC superfamily's signature residues

In order to identify and study critical residues involved in NMN deamidation reaction, we performed a large multiple sequence analysis with over 500 PncC sequences (see Fig. S1). Fig. 1 shows an alignment of 30 most divergent sequences, including the proteins from *E. coli* and *Shewanella oneidensis*, which have been experimentally characterized by us [7], and the protein from *A. tumefaciens*, whose 3D structure is available. This allowed us to identify three signature motifs: ESxTxG, YxxxxK, and (S/T)GxA; additionally, an arginine residue appears to be invariably conserved in all analyzed sequences (Fig. 1). The abundance of serine and threonine residues among the conserved residues, in combination with previous inhibition studies ruling out a thiol- or metal-dependent type of amidohydrolase [7], suggested that PncC might employ one of the diverse active site configurations described for serine/threonine proteases. We next carried out site-directed mutagenesis to identify critical catalytic residues.

3.2. Identification of critical residues by site-directed mutagenesis

Among the 10 highly conserved residues spotted by the sequence alignment analysis, 7 amino acids were selected for site-directed mutagenesis based on their potential ability to participate in acid/base chemistry and/or hydrogen bonding (Fig. 1). *E. coli* PncC (*ec*PncC) was used as the template to generate the following mutated proteins: E28A, S29A, T31A, Y56A, K61Q, S103A and R142A. Mutants were overexpressed in *E. coli* cells, and purified to

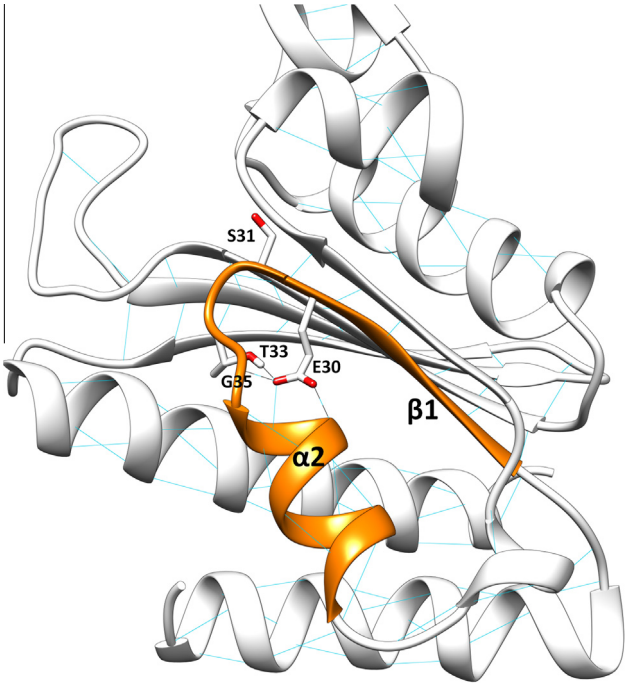

Fig. 3. Crystal structure of the *at*PncC monomer, highlighting the role of E30, T33 and G35 in α2-loop-β1 clamping, which contributes to S31 nucleophile orientation.

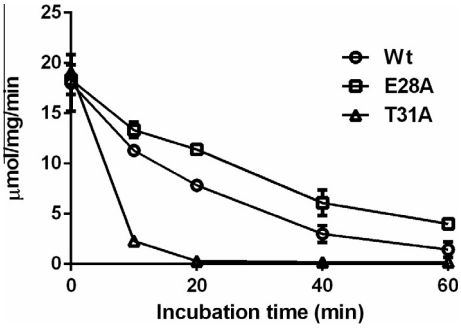

Fig. 4. Residual enzymatic activity of purified wild type PncC, E28A, and T31A mutants after incubation at 70 °C at the indicated times. Enzymatic activity was assayed as described in Section 2.

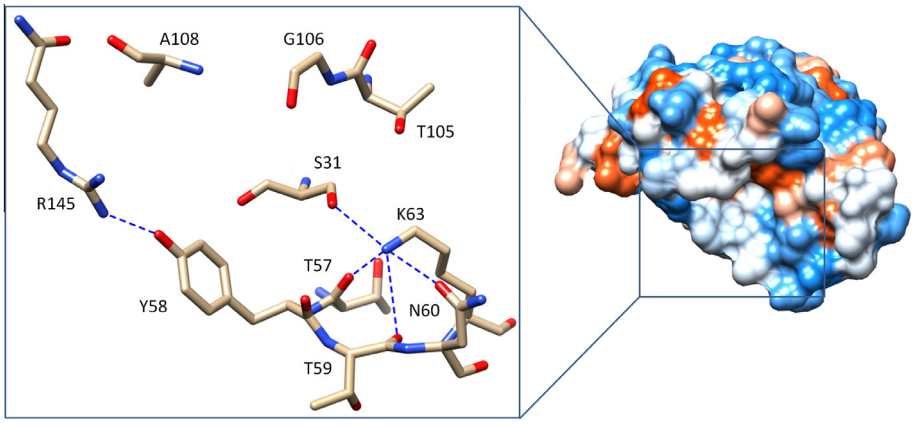

Fig. 2. Electrostatic surface of the *PncC* monomer from *Agrobacterium tumefaciens* (PDB code 2A9S), with close-up view of the active site. Residues conserved in the PncC sequence, and residues potentially H-bonded to the proposed K63 catalytic base are evidenced. H-bonds are represented by dashed lines.

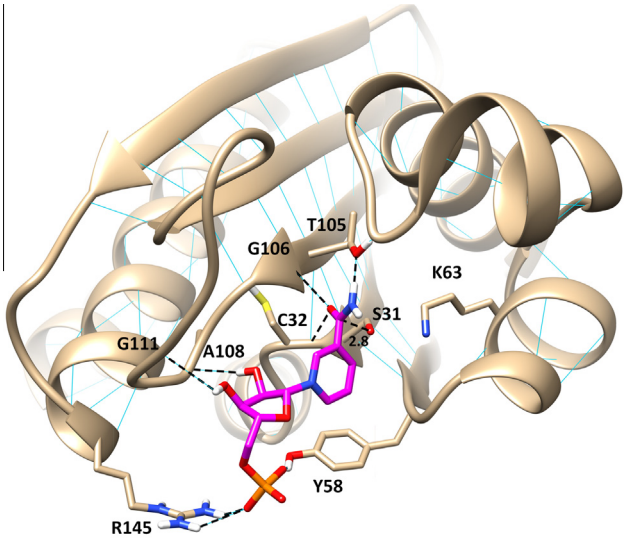

Fig. 5. Detailed view of *at*PncC active site with a modeled NMN molecule. Residues that are likely to engage H-bonding with the ligand are evidenced, including the residues G106 and C32 predicted to form the oxyanion hole. Hydrogen bonds are shown as dashed lines. The catalytic residue K63 is also evidenced.

homogeneity, as described in Section 2. SDS–PAGE of purified enzymes showed that all mutants were expressed as soluble proteins, migrating at the same position (about 19 kDa) as the wild type (not shown).

A detailed kinetic analysis of the purified proteins showed that S29A, Y56A, K61Q, and R142A mutants completely lost catalytic activity (Table 1). Compared to wild-type enzyme, T31A and S103A exhibited a 5- and 7-fold lower catalytic efficiency, respectively, and replacement of E28 with alanine yielded a 60-fold decrease. Notably, while in T31A and E28A mutants only the substrate affinity was affected (4 and 40-fold increase in K_m, respectively), in the S103A mutant the k_{cat}/K_m reduction was mainly due to k_{cat} impairment (Table 1). These results suggest that T31 and E28 might play a structural role rather than a catalytic one, while S103 is likely involved in catalysis.

3.3. Defining the active site configuration of PncC superfamily: the catalytic core

Among the seven absolutely conserved residues whose involvement in catalysis has been assessed by our mutagenesis experiments, five are located in the putative active site that we have previously predicted [7], based on surface charge analysis and substrate docking performed on the available PncC structure from *A. tumefaciens* (*at*PncC, PDB code 2A9S) (Fig. 2). The presence in the active site of a serine residue essential for catalysis (S31, corresponding to S29 in *ec*PncC) strongly suggests that PncC might be a serine amidohydrolase. Since most serine hydrolases are inhibited by electrophilic compounds known to covalently modify the nucleophile [18,19], we tested the effect of PMSF and a fluorophosphonate on the PncC activity. The results showed that the compounds were not able to inhibit the enzyme activity, indicating that PncC does not behave as a "classic" serine hydrolase. However, some serine hydrolases have been described which are not affected by fluorophosphonates and sulfonyl fluoride inhibitors, despite possessing a serine nucleophile, including signal peptidase [20] and a few members of the "amidase signature" superfamily [4,21].

Inspection of residues surrounding the proposed S31 nucleophile in *at*PncC structure identified K63 (K66 in *ec*PncC) as the only coordination partner at H-bonding distance (2.9 Å) (Fig. 2). This observation, together with the lysine's essential role in catalysis, as demonstrated by the mutagenesis experiments, makes it a strong candidate to function as the general base, capable of directly activating S31 for catalysis by increasing its nucleophilicity. Although the network of H-bonding acceptors surrounding K63 in the crystal structure (Fig. 2) would support a protonated state for K63, it is plausible that the substrate binding would promote the deprotonated state of the catalytic lysine, as required for serine nucleophile activation. Taken together, these observations indicate that the PncC superfamily employs a Ser/Lys dyad for catalysis.

Ser/Lys amidohydrolases represent a wide group of enzymes with different folds and biological functions. They include proteases, i.e. signal peptidases [8,9,22,23], Lon protease [24], C-terminal processing peptidases [25], proteases of the UmuD family [8,26], penicillin binding proteins [27], viral proteases [28], lactoferrin [29], and amidases like β-lactamase [30] and glutaminase [10,11]. The common mechanistic trait of Ser/Lys amidohydrolases is the nucleophilic attack by the serine hydroxyl aided by a lysine ε-amine acting as the general base. However, in a number of cited cases, i.e. in the evolutionary related penicillin binding proteins and β-lactamases, auxiliary catalytic players are required [31,32].

Our discovery that PncC is an amidohydrolase employing a Ser/Lys catalytic dyad expands the repertoire of amidases with similar active site architecture and different overall fold, and is in keeping with the concept that the Ser/Lys dyad active site arrangement has arisen multiple times, as a result of convergent evolution [6,33].

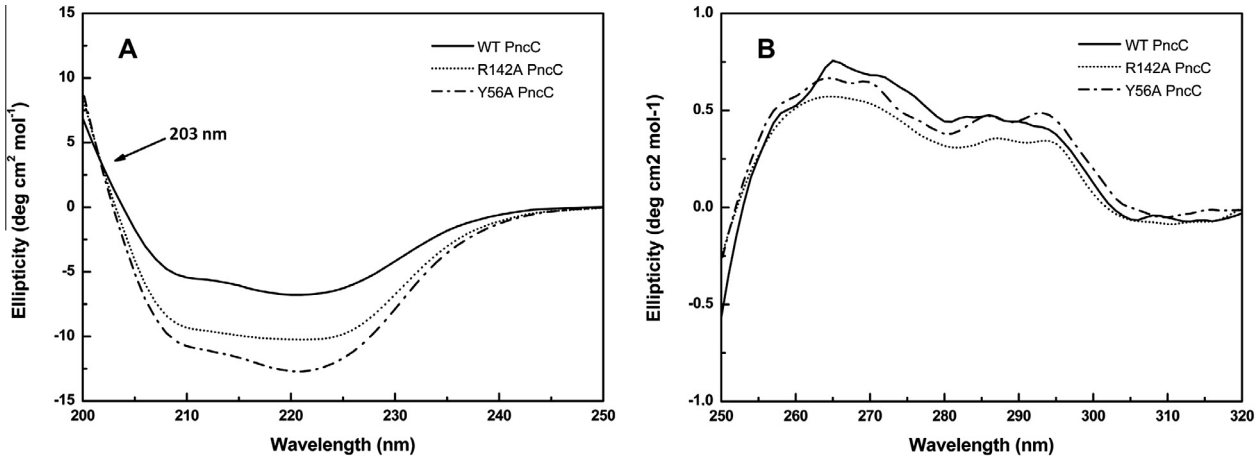

Fig. 6. Circular dichroism spectra in the far-UV (A) and near-UV (B) of wild type PncC, Y56A, and R142A. Spectra were recorded at 25 °C as detailed in Section 2. Isodichroic point in the far-UV spectrum is indicated by a solid arrow.

3.4. Defining the active site configuration of PncC superfamily: residues surrounding the catalytic core

In order to understand the role of the other residues whose substitution was found to affect PncC catalytic efficiency, we next focused on the conserved E30 and T33 residues (E28 and T31 in *ec*PncC) of the ESxTxG signature sequence (Fig. 1). The kinetic characterization of the mutated proteins showed that the replacement of glutamate with alanine yields a 60-fold decrease in the k_{cat}/K_m value, while T31A mutation resulted in only a 5-fold reduction (Table 1). Notably, these effects are essentially due to a decrease in the affinity for the substrate (Table 1). Inspection of the structural localization of these residues revealed that, despite being adjacent to the catalytic serine in the primary structure, both of them point away from the enzyme catalytic center (Fig. 3). E30, that resides in the β1 strand, interacts with α2 helix, whereas T33 helps orienting E30 itself through an H-bond. These results suggest a structural, rather than catalytic function. Such a role is also evidenced by the results of thermal stability experiments performed on the mutants. As shown in Fig. 4 both mutations clearly affect the enzyme thermal stability which is severely reduced in T31A and significantly increased in E28A.

Similarly to T33, the conserved G35 of the ESxTxG signature, not mutated in this work, is H-bonded to E30 through its main chain (Fig. 3).Therefore these three residues appear to lock β1 strand and α2 helix together, thus contributing to the correct orientation of the serine nucleophile that resides in the connecting loop (Fig. 3).

We have previously reported the *at*PncC structure in complex with a NMN molecule modeled into the predicted active site [7]. The substrate pose in the active site has been recently confirmed by Sánchez-Carrón et al. [34]. Interestingly, the modeled substrate is found to interact with all the conserved residues demonstrated to be critical for PncC catalysis and located in the active site (Fig. 5). In particular, the extended conformation (with no intramolecular H-bonds) adopted by NMN seems to favor the attack of the S31 nucleophile to the carbonyl of the scissile bond. In addition, T105 (S103 in *ec*PncC) might contribute to the correct

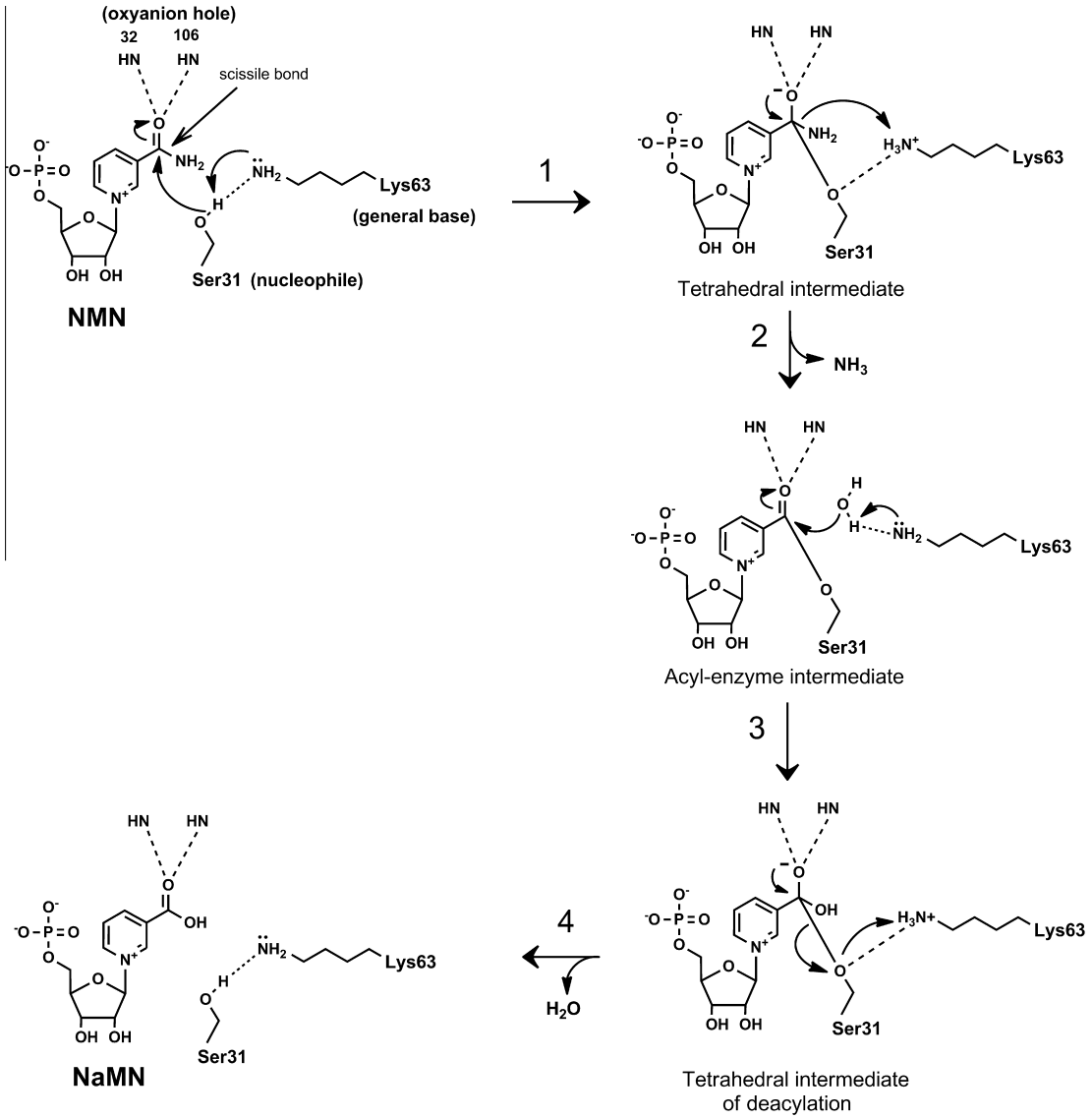

Fig. 7. Proposed mechanism of NMN deamidation catalyzed by PncC. The reaction proceeds through the following steps: (1) nucleophilic attack of the S31 oxygen to form the tetrahedral intermediate; (2) decomposition of the tetrahedral intermediate with the production of acyl-enzyme intermediate and release of ammonia; (3) nucleophilic attack of a deacylating water molecule; (4) release of the second product (NaMN) and free enzyme.

orientation of NMN amide group for catalysis (Fig. 5), in agreement with its non-essential role, as evidenced by the mutagenesis experiments.

Mutagenesis studies showed that two additional residues located in the active site were essential for the enzyme activity, i.e. Y58 and R145 (Y56 and R142 in *ec*PncC) (Table 1). In order to assess whether the loss of catalytic activity is caused by disruption of the active site architecture we performed CD analysis on the two purified mutants and wild type PncC (Fig. 6). The secondary structures were investigated by far-UV CD, and the obtained spectra (Fig. 6A) were analyzed by the Yang's algorithm [35]. The results show a remarkable increase of the percentage of random structure in R142A and Y56A (from 3% to 12% and 9%, respectively) with a decrease of their α-helices content (data not shown). In addition, the far-UV CD spectra show the presence of an isodichroic point at 203 nm (Fig. 6A), indicative of an α-helix to random coil transition for both mutants [36]. The tertiary structural organization was investigated by CD spectra in the near-UV region. Wild type PncC shows a well structured spectrum in the aromatic region, suggesting the presence of an extended network of intramolecular interactions in the three-dimensional matrix of the protein (Fig. 6B). The mutant Y56A presents a well structured near-UV spectrum in which is clearly visible the diminution of Tyr contribution at 278 nm. On the contrary, the near-UV spectrum of R142A (Fig. 6B) appears to be less structured indicating a different finger print of the protein side-chains [37]. Overall, these conformational changes may explain the loss of enzyme activity by the mutant proteins.

In the solved apo-structure of *at*PncC, Y58 and R145 are H-bonded (Fig. 2), whereas in our docked structure with NMN they move away from each other, beyond H-bonding distance, and appear to stabilize the phosphate moiety of the substrate (Fig. 5).

In addition, our modeled structure allowed us to assign a possible role also to the two conserved residues G106 and A108, not mutated in this study. Both residues are located in the active site (Fig. 2) and A108 main chain seems to engage an H-bond with the 2′-hydroxyl of the ribosyl moiety of NMN, favoring substrate binding, while G106 main chain appears to polarize the nicotinyl carbonyl oxygen, favoring the nucleophilic attack (Fig. 5).

Overall, our data show that all the conserved and critical residues included in the three signature motifs (Fig. 1) play distinct roles in catalysis or substrate binding.

3.5. Proposed model for the chemical mechanism of hydrolytic cleavage

Our structural and mutagenesis results support a catalytic Ser/Lys dyad mechanism, as shown in Fig. 7. According to this model, the ε-amino group of K63 acts as the general base, and extracts a proton from the hydroxyl group of S31. This activation prepares S31 for the nucleophilic attack of the carbonyl carbon of the scissile amide bond of the nicotinamide moiety which results in the formation of the oxyanion tetrahedral intermediate. The latter is stabilized by the oxyanion hole likely formed from the main-chain amides of C32 and G106 (Fig. 5). Catalysis then proceeds through the formation and subsequent cleavage of the covalent acyl-enzyme intermediate as described in Fig. 7. Validation of the proposed PncC catalytic mechanism awaits the 3D structure resolution of the enzyme with bound substrate or inhibitor.

In conclusion, the results from mutagenesis experiments combined with the structural analysis of both the PncC apoenzyme and its form in complex with a modeled NMN molecule, allowed us to define the active site of PncC and assign specific roles to all conserved residues. This revealed that PncC is a Ser/Lys amidohydrolase: its unique function (nucleotide deamidase) and fold expand the diversity of this large group of amidohydrolases.

Acknowledgments

This work was partly supported by the Italian Ministry of Foreign Affairs, "Direzione Generale per la Promozione del Sistema Paese" to N.R and by the "Montalcini International Program Grant" through the Italian Ministry of Education, University, and Research to L.S.

Appendix A. Supplementary data

Supplementary data associated with this article can be found, in the online version, at http://dx.doi.org/10.1016/j.febslet.2014.01.063.

References

[1] Seibert, C.M. and Raushel, F.M. (2005) Structural and catalytic diversity within the amidohydrolase superfamily. Biochemistry 44, 6383–6391.
[2] Nguyen, J.T., Hamada, Y., Kimura, T. and Kiso, Y. (2008) Design of potent aspartic protease inhibitors to treat various diseases. Arch. Pharm. (Weinheim) 341, 523–535.
[3] Dodson, G. and Wlodawer, A. (1998) Catalytic triads and their relatives. Trends Biochem. Sci. 23, 347–352.
[4] Labahn, J., Neumann, S., Buldt, G., Kula, M.R. and Granzin, J. (2002) An alternative mechanism for amidase signature enzymes. J. Mol. Biol. 322, 1053–1064.
[5] Shin, S., Yun, Y.S., Koo, H.M., Kim, Y.S., Choi, K.Y. and Oh, B.H. (2003) Characterization of a novel Ser-*cis*Ser-Lys catalytic triad in comparison with the classical Ser-His-Asp triad. J. Biol. Chem. 278, 24937–24943.
[6] Ekici, O.D., Paetzel, M. and Dalbey, R.E. (2008) Unconventional serine proteases: variations on the catalytic Ser/His/Asp triad configuration. Protein Sci. 17, 2023–2037.
[7] Galeazzi, L. et al. (2011) Identification of nicotinamide mononucleotide deamidase of the bacterial pyridine nucleotide cycle reveals a novel broadly conserved amidohydrolase family. J. Biol. Chem. 286, 40365–40375.
[8] Paetzel, M. and Strynadka, N.C. (1999) Common protein architecture and binding sites in proteases utilizing a Ser/Lys dyad mechanism. Protein Sci. 8, 2533–2536.
[9] Paetzel, M., Dalbey, R.E. and Strynadka, N.C. (2002) Crystal structure of a bacterial signal peptidase apoenzyme: implications for signal peptide binding and the Ser-Lys dyad mechanism. J. Biol. Chem. 277, 9512–9519.
[10] Yoshimune, K., Shirakihara, Y., Shiratori, A., Wakayama, M., Chantawannakul, P. and Moriguchi, M. (2006) Crystal structure of a major fragment of the salt-tolerant glutaminase from *Micrococcus luteus* K-3. Biochem. Biophys. Res. Commun. 346, 1118–1124.
[11] Brown, G. et al. (2008) Functional and structural characterization of four glutaminases from *Escherichia coli* and *Bacillus subtilis*. Biochemistry 47, 5724–5735.
[12] Overbeek, R. et al. (2005) The subsystems approach to genome annotation and its use in the project to annotate 1000 genomes. Nucleic Acids Res. 33, 5691–5702.
[13] Edgar, R.C. (2004) MUSCLE: multiple sequence alignment with high accuracy and high throughput. Nucleic Acids Res. 32, 1792–1797.
[14] Cialabrini, L., Ruggieri, S., Kazanov, M.D., Sorci, L., Mazzola, F., Orsomando, G., Osterman, A.L. and Raffaelli, N. (2013) Genomics-guided analysis of NAD recycling yields functional elucidation of COG1058 as a new family of pyrophosphatases. PLoS ONE 8, e65595.
[15] Gouet, P., Robert, X. and Courcelle, E. (2003) ESPript/ENDscript: extracting and rendering sequence and 3D information from atomic structures of proteins. Nucleic Acids Res. 31, 3320–3323.
[16] Kitagawa, M., Ara, T., Arifuzzaman, M., Ioka-Nakamichi, T., Inamoto, E., Toyonaga, H. and Mori, H. (2005) Complete set of ORF clones of *Escherichia coli* ASKA library (a complete set of *E. coli* K-12 ORF archive): unique resources for biological research. DNA Res. 12, 291–299.
[17] Laemmli, U.K. (1970) Cleavage of structural proteins during the assembly of the head of bacteriophage T4. Nature 227, 680–685.
[18] Patricelli, M.P., Lovato, M.A. and Cravatt, B.F. (1999) Chemical and mutagenic investigations of fatty acid amide hydrolase: evidence for a family of serine hydrolases with distinct catalytic properties. Biochemistry 38, 9804–9812.
[19] Liu, Y., Patricelli, M.P. and Cravatt, B.F. (1999) Activity-based protein profiling: the serine hydrolases. Proc. Natl. Acad. Sci. USA 96, 14694–14699.
[20] Zwizinski, C., Date, T. and Wickner, W. (1981) Leader peptidase is found in both the inner and outer membranes of *Escherichia coli*. J. Biol. Chem. 256, 3593–3597.

[21] Koo, H.M., Choi, S.O., Kim, H.M. and Kim, Y.S. (2000) Identification of active-site residues in *Bradyrhizobium japonicum* malonamidase E2. Biochem. J. 349, 501–507.
[22] Paetzel, M., Karla, A., Strynadka, N.C. and Dalbey, R.E. (2002) Signal peptidases. Chem. Rev. 102, 4549–4580.
[23] Kim, A.C., Oliver, D.C. and Paetzel, M. (2008) Crystal structure of a bacterial signal peptide peptidase. J. Mol. Biol. 376, 352–366.
[24] Rotanova, T.V., Melnikov, E.E., Khalatova, A.G., Makhovskaya, O.V., Botos, I., Wlodawer, A. and Gustchina, A. (2004) Classification of ATP-dependent proteases Lon and comparison of the active sites of their proteolytic domains. Eur. J. Biochem. 271, 4865–4871.
[25] Liao, D.I., Qian, J., Chisholm, D.A., Jordan, D.B. and Diner, B.A. (2000) Crystal structures of the photosystem II D1 C-terminal processing protease. Nat. Struct. Biol. 7, 749–753.
[26] Peat, T.S., Frank, E.G., McDonald, J.P., Levine, A.S., Woodgate, R. and Hendrickson, W.A. (1996) Structure of the UmuD' protein and its regulation in response to DNA damage. Nature 380, 727–730.
[27] Davies, C., White, S.W. and Nicholas, R.A. (2001) Crystal structure of a deacylation-defective mutant of penicillin-binding protein 5 at 2.3-Å resolution. J. Biol. Chem. 276, 616–623.
[28] Feldman, A.R., Lee, J., Delmas, B. and Paetzel, M. (2006) Crystal structure of a novel viral protease with a serine/lysine catalytic dyad mechanism. J. Mol. Biol. 358, 1378–1389.
[29] Anderson, B.F., Baker, H.M., Norris, G.E., Rice, D.W. and Baker, E.N. (1989) Structure of human lactoferrin: crystallographic structure analysis and refinement at 2.8 Å resolution. J. Mol. Biol. 209, 711–734.
[30] Massova, I. and Mobashery, S. (1998) Kinship and diversification of bacterial penicillin-binding proteins and beta-lactamases. Antimicrob. Agents Chemother. 42, 1–17.
[31] Pratt, R.F. and McLeish, M.J. (2010) Structural relationship between the active sites of beta-lactam-recognizing and amidase signature enzymes: convergent evolution? Biochemistry 49, 9688–9697.
[32] Adediran, S.A., Lin, G., Pelto, R.B. and Pratt, R.F. (2012) Crossover inhibition as an indicator of convergent evolution of enzyme mechanisms: a beta-lactamase and a N-terminal nucleophile hydrolase. FEBS Lett. 586, 4186–4189.
[33] Gherardini, P.F., Wass, M.N., Helmer-Citterich, M. and Sternberg, M.J. (2007) Convergent evolution of enzyme active sites is not a rare phenomenon. J. Mol. Biol. 372, 817–845.
[34] Sanchez-Carron, G., Martinez-Monino, A.B., Sola-Carvajal, A., Takami, H., Garcia-Carmona, F. and Sanchez-Ferrer, A. (2013) New insights into the phylogeny and molecular classification of nicotinamide mononucleotide deamidases. PLoS ONE 8, e82705.
[35] Yang, J.T., Wu, C.S. and Martinez, H.M. (1986) Calculation of protein conformation from circular dichroism. Methods Enzymol. 130, 208–269.
[36] Gazi, A.D., Bastaki, M., Charova, S.N., Gkougkoulia, E.A., Kapellios, E.A., Panopoulos, N.J. and Kokkinidis, M. (2008) Evidence for a coiled–coil interaction mode of disordered proteins from bacterial type III secretion systems. J. Biol. Chem. 283, 34062–34068.
[37] D'Auria, S., Rossi, M., Nucci, R., Irace, G. and Bismuto, E. (1997) Perturbation of conformational dynamics, enzymatic activity, and thermostability of beta-glycosidase from archaeon *Sulfolobus solfataricus* by pH and sodium dodecyl sulfate detergent. Proteins 27, 71–79.